Mutual Coupling Suppression Between Two Closely Placed Patch Antennas Using Higher-Order Modes

Jian-Feng Qian, *Graduate Student Member, IEEE*, Steven Gao, *Fellow, IEEE*, Benito Sanz-Izquierdo, *Member, IEEE*, Hanyang Wang, *Fellow, IEEE*, Hai Zhou, and Huiliang Xu

***Abstract*— This article presents a novel method for decoupling two patch antennas. Instead of using the TM_{10} mode of a conventional patch, TM_{20} mode is utilized as the operation mode of the antenna. By loading stubs at the radiating edge of the patch, the resonance frequency of the TM_{20} mode is moved down to the same band as the original TM_{10} mode. Then, the mutual coupling between two such patch antennas is suppressed simply by physical placement, even when they are placed extremely close to each other. Without using any extra decoupling elements, isolation is improved by up to 20 dB using this method. Furthermore, this method can also be applied to multielement multi-input -multi-output (MIMO) array and dual-antenna system with different operating bands. The proposed method is verified with three different application scenarios, including a two-element MIMO array, a two-antenna system with adjacent operating bands, and a four-element MIMO array. Reasonable agreements between simulated and measured results can be observed, showing the advantages of simple structure, low cost, high isolation, and good radiation performance.**

***Index Terms*— Adjacent band, in-band, multi-input-multi-output (MIMO), mutual coupling, patch antenna.**

I. Introduction

OVER the decades, the mutual coupling suppression between two antennas has drawn much attention among academic and industrial communities. The mutual coupling problem is believed to be one of the critical bottlenecks for two technologies. The first one is well-known multi-input-multi-output (MIMO) technology. By using MIMO technology, the throughput of the wireless communication system can be increased dramatically. The channel capacity of the MIMO array can be multiplied with more antenna elements involved theoretically. However, the limited performance of the MIMO system may be observed if the mutual coupling and spatial correlation are not suppressed to an adequately low level [1]. The second technology is called in-band full-duplex (IBFD) technology [2]. Unlike time-division duplex (TDD) and frequency-division duplex (FDD) technologies, IBFD allows the transmitter and receiver to operate over the same frequency band simultaneously. To ensure the system's performance, the signal interferences between two channels should be as low as possible to avoid saturation of the analog-to-digital/digital-to-analog converter (ADDA). Although some of these problems can be accommodated in the analog and digital domain after the antennas, the impact of mutual coupling can never be underestimated.

Patch antenna now has been the most popular candidate for the next-generation wireless communication technology for its feather of low profile, low cost, ease of mass production, and ease of integrating with other circuits. It is also widely used for millimeter-wave (mm-Wave) band applications, such as 5G mobile communication and automotive radars. As a result, the mutual coupling problem between patch antennas is becoming increasingly important. Due to the limited space, it is not realizable to increase the isolation between antenna elements by moving them away from each other. To address this problem, many efforts have been made by researchers.

A common method is to introduce additional parasitic elements with a band-reject response between coupled antennas [3], [4]. Most of these band-reject structures can only provide a transmission null in a narrow frequency band. In addition, the loading elements sometimes also strongly affect the antennas' radiation and impedance performance. Another technique is using artificial structures [5], [6], [7]. However, to the best of our knowledge, most of these artificial surfaces and apertures occupy a considerable printed circuit board (PCB) area. If they are placed between antenna elements, then additional space must be reserved for implementing these structures [6]. If they are mounted over the antenna elements, additional circuit layers are needed depending on the layers of the decoupling structures [7]. This will not only increase the system profile but also increase the cost.

Decoupling network is another option for mutual coupling suppression [8], [9], [10], [11], [12], [13], [14]. These networks can be designed using lumped elements [8], [9] or distributed structures [10], [11], [12], [13], [14]. In [10], by studying the *Y*- matrix of coupled antennas, a novel dual-band decoupling network is presented. In [11], power-dividing networks and filters are adopted for the

Manuscript received 16 November 2022; revised 15 February 2023; accepted 3 March 2023. Date of publication 10 April 2023; date of current version 2 June 2023. This work was supported in part by Huawei Technology Ltd., in part by the Engineering and Physical Sciences Research Council (EPSRC) under Grant EP/S005625/1, and in part by the Royal Society-International Exchanges 2019 Cost Share (NSFC) under Grant IEC/NSFC/191780. *(Corresponding author: Jian-Feng Qian.)*

Jian-Feng Qian and Benito Sanz-Izquierdo are with the School of Engineering and Digital Arts, University of Kent, CT2 7NT Canterbury, U.K. (e-mail: jq42@kent.ac.uk).

Steven Gao is with the Department of Electronic Engineering, The Chinese University of Hong Kong, Hong Kong.

Hanyang Wang, Hai Zhou, and Huiliang Xu are with Huawei Technology Ltd., RG2 6UF Reading, U.K.

Color versions of one or more figures in this article are available at https://doi.org/10.1109/TAP.2023.3264874.

Digital Object Identifier 10.1109/TAP.2023.3264874

design of high-performance decoupling structures. In [12], a transmission-line-based decoupling network is introduced for MIMO applications. In [13], by placing a bandstop filter between two patch antennas, an improvement of 28 dB can be achieved. Generally, the performance of these decoupling networks is related to the complexity of the design. As a result, some of these designs suffer from high loss [8], large decoupling size, and time-consuming design procedures [11], [12], [13]. Another option for achieving multiple isolated channels is through the use of shared-radiator antennas as reported in [15], [16], [17], and [18]. In these solutions, all the antennas share a common radiator. The isolation between ports is accomplished by utilizing different modes of the radiator [15], [16], common mode and differential mode cancellation [17], and additional decoupling structure [18].

Some compact solutions for low-profile decoupling realizations can also be found in the literature by utilizing the inherent characteristic of patch antennas [19], [20], [21]. Lin et al. [19] present a self-decoupling method by investigating the field distributions at an insert-fed patch antenna. By placing one antenna element at the inherent weak field region caused by the feeding structure of another antenna, two antennas can be isolated without using any decoupling structure. Unfortunately, the long feeding structure limits the minimum achievable distance between every two antennas and their application scenarios. Another interesting work is presented in [20]. In the work, the transversal mode of a wide patch is excited together with the fundamental mode TM_{10} mode to construct a null-field region at the other antenna, such that the mutual coupling can be suppressed. The disadvantage of this method is that it can only decouple two identical antennas and wide patches are necessary to move the frequency of TM_{02} mode to be close to the one of the TM_{10} mode.

Another problem with these decoupling methods is that most of them are very sensitive to the symmetry of the antennas to be decoupled and are only verified effective for two identical antennas. However, the decoupling problem between two different antennas is also very important [22], [23], [24]. For a commercial device supporting different standards for different regions, multiple antennas operating over different frequency bands must be well-isolated. When it comes to this case, most of the presented methods may not be effective anymore.

In this article, a novel decoupling method is presented. Using this method, two very closely placed patch antennas are decoupled without needing additional decoupling structure. Instead of using a conventional rectangular patch operating under its fundamental TM_{10} mode, stub-loaded patches with modified TM_{20} modes are used as the basic antenna elements to be decoupled. The mutual coupling between two such two patch antennas is suppressed simply and effectively by placing them with a proper offset along their polarization direction. This has been realized by investigating the field distributions along the nonradiating edges of the TM_{20} mode. The detailed working mechanism will be explained in the case of two probe feed patch antennas and verified with three different experimental examples. Through our study, this novel decoupling concept has the following attractive advantages.

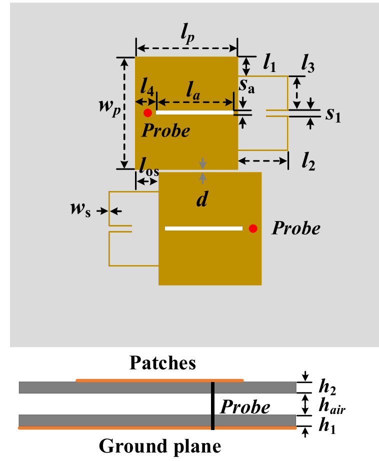

Fig. 1. Dimensions of the dual-antenna system (unit: mm): $l_1 = 3.8$, $l_2 = 6.65$, $l_3 = 7.7$, $l_4 = 3.375$, $l_{os} = 5.2$, $l_p = 22.15$, $w_s = 0.3$, $w_p = 23.2$, $S_a = 1$, $l_a = 18$, $d = 0.4$, $h_1 = 0.813$, $h_2 = 0.813$, and $h_{air} = 2$.

1) It is insensitive to patch separation. So, it can be applied to two extremely closely placed patch antennas.
2) No additional decoupling structure or layer is needed. The decoupling concept and structure are very simple but effective. Thus, the design process is very easy and quick.
3) It can also be applied to two patch antennas operating at two different frequency bands.
4) It has little influence on the radiation and impedance performance of the patch antenna, which means this method will also be helpful for large-scale phase arrays.

This article is organized as follows. First, in Section II, a dual-antenna system composed of identical probe-fed patch antennas is designed to validate the idea. The working mechanism of the proposed decoupled method is explained by investigating the field distributions of the patch antennas. Some parametric studies are carried out to help understand the proposed idea better. Then, in Section III, the effectiveness of the proposed method for the adjacent-band and four-element MIMO applications is studied and discussed. All the cases are verified with experimental results, showing good impedance bandwidths and low mutual coupling levels.

II. Decoupling for In-Band Operation

A. Basic Physical Structure

Fig. 1 shows the structure of the dual-antenna system for demonstration in this article. It consists of two substrates, which are all Rogers 4003 with a dielectric constant of 3.55 and thickness of 0.813 mm. Between the substrates, a 2 mm air gap is introduced to improve the bandwidths and efficiencies of the antennas [25]. Note that the technique described here provides a similar decoupling level when no air gap is present, and the antenna is lower in profile (e.g., a total height of 0.813 mm). The radiators are placed on the top substrate's upper surface, and the common ground plane is located on the lower surface of the bottom substrate. Slotted stub-loaded patches are used as radiators. A classical probe-feeding structure is used for the excitations of these antennas. All the probes used in this work have a diameter of 0.7 mm.

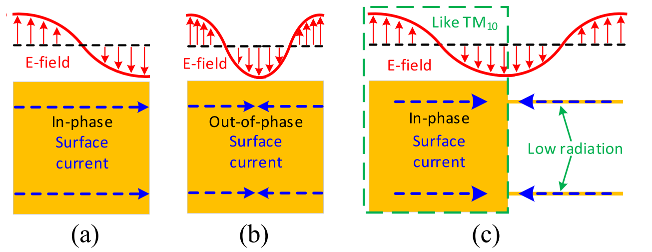

Fig. 2. E-field and surface current distributions. (a) TM_{10} mode and (b) TM_{20} mode of a conventional patch antenna. (c) TM_{20} mode of a stub-loaded patch antenna.

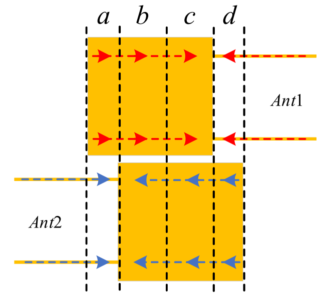

Fig. 3. Conceptual diagram for the current distributions for the dual-antenna system.

In contrast to previous works in the literature which study classical rectangular patches, stub-loaded patches are used here as the antenna elements. It is well-known that the fundamental TM_{10} mode of a rectangular patch shows half-wavelength standing wave distribution along its nonradiating edges, as shown in Fig. 2(a). The in-phase fringe fields at their two radiating edges ensure a good broadside radiation characteristic. When two such antennas are placed very close to each other, the mutual coupling between these two antennas will be very strong, resulting in deteriorated radiation and impedance performances.

The original TM_{20} mode of a patch antenna has a radiation null in its broadside direction due to out-of-phase current distributions at its two radiating edges, as shown in Fig. 2(b). In this work, to circumvent this problem, two open-ended stubs are loaded onto one of the radiating edges. This results in the reconfiguration of the field distribution beneath the patch, leading to in-phase current distributions at the open ends and a shift in the frequency band of the TM_{20} mode, as illustrated in Fig. 2(c). Besides, because the stubs are too narrow to radiate effectively, the TM_{20} mode demonstrates improved broadside radiation characteristic, which is similar to the TM_{10} mode. This phenomenon can be observed in some other presented works [26], [27], [28], [29].

By increasing the length of the stub, the resonant frequency of the TM_{20} mode can be moved to the same frequency band as the original TM_{10} mode. Compared with other presented works in which shorter stubs are used [26], [27], [28], [29], here, the stub is longer, such that the TM_{10} mode is suppressed by the band-reject response introduced by the open-ended stubs [26]. If two such antennas are placed very close to each other, very high isolation can be achieved by simply introducing an offset along its nonradiating edges. This is described in Section II-B.

B. Decoupling Mechanism

To get an insight into the working mechanism of the proposed method, the field distributions on the patches are shown in Fig. 3. As can be seen, when two TM_{20} mode-based patch antennas are placed closely, the field distributions along the nonradiating edges, which is also the area where coupling occurs, can be divided into four regions. In regions a and d, the current vectors on both antennas are in phase, whereas in regions b and c, the currents are out of phase. By deliberately designing the offset along the polarization direction to control the weight of each region, the mutual coupling related to region a will cancel the counterparts dominated by region b. A similar result can be found for regions c and d. Then, mutual coupling can be suppressed dramatically by optimizing the offset between these two antennas.

To further understand the working mechanism of this method, some key parameters are studied. To ensure a fair comparison, the other dimensions are all kept as the values given in Fig. 1 when one parameter is studied. The simulations are all carried out using high-frequency structure simulator (HFSS) [30].

The responses with different offsets (l_{os}) are plotted in Fig. 4(a). As the offset between two antennas increases, the null of mutual coupling shifts to the lower band. Regarding the frequency band of interest, the offset strongly affects the in-band mutual coupling level, which corresponds with the theoretical analysis. A slight frequency shift can also be observed when the offset changes because of the variation of the loading effect between two antennas. It can be observed that the null on S_{21} can be controlled by adjusting the offset distance (l_{os}) between two patches. A properly designed offset can move the transmission null to the frequency band, where the patch is resonant, so that two antennas can be decoupled.

Once the location of the null is shifted to the desired location, good suppression can be achieved by optimizing the weight of different regions as indicated in Fig. 3. As the contribution of regions b and c to the total mutual coupling is mainly decided by the distance between two antennas, another critical parameter that dominates the mutual coupling suppression is the location of the stub (l_1). The coupling strength related to regions a and d in Fig. 3 is highly related to the distance between the stub of one antenna to the nonradiating edge of the other antenna. By adjusting the locations of the stubs, the mutual coupling dominated by regions a and d will neutralize the counterpart related to regions b and c. Fig. 4(b) shows the effect of the stub location on the mutual coupling. By varying the location of the stub, the depth of the null on S_{21} can be improved, so that higher isolation can be obtained. Together with Fig. 4(a), the mutual coupling between two patches can be decreased by adjusting the offset between patches (l_{os}) and the locations of the stubs (l_1). These two parameters are the key factors, which have the strongest effect on the decoupling performance.

One interesting fact that needs to be emphasized is that this decoupling method can handle the mutual coupling problem of

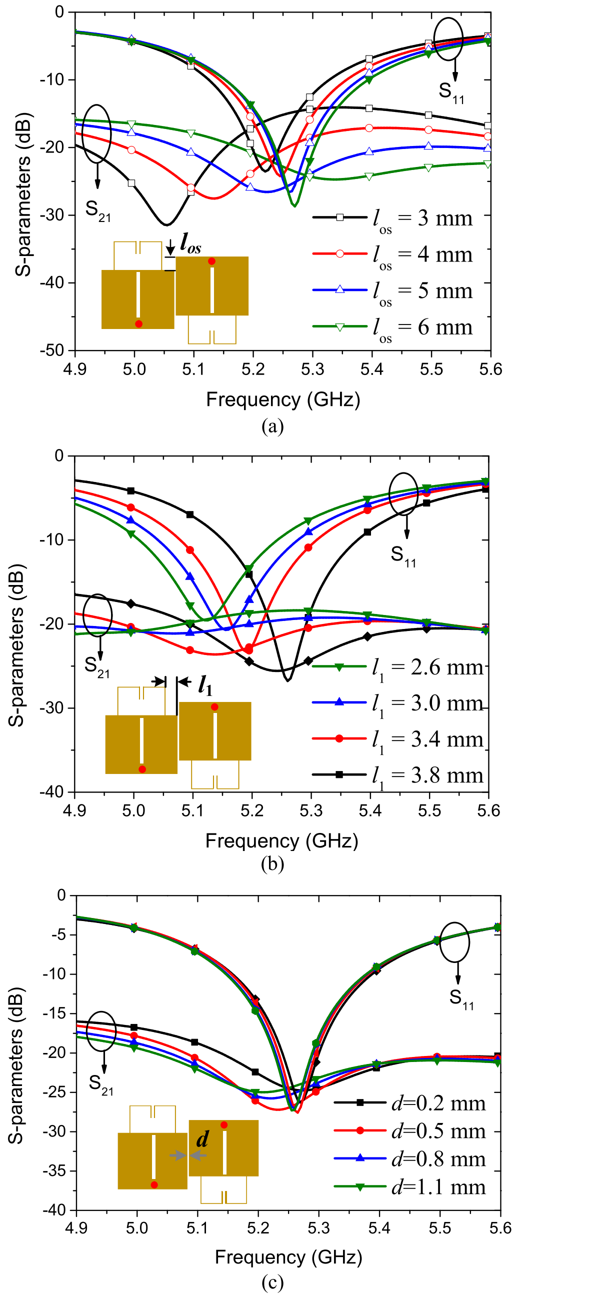

Fig. 4. Simulated S-parameters with different (a) offsets (l_{os}), (b) stub locations (l_1), and (c) antenna distances (d).

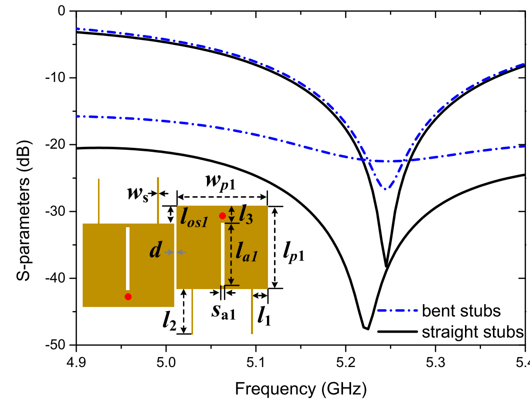

Fig. 5. Comparison on the S-parameters of the designs with bent and straight stubs. Dimensions of the antennas with straight stubs in mm: $l_1 = 4$, $l_2 = 16.15$, $l_3 = 3.375$, $l_{os1} = 5$, $l_{p1} = 22.2$, $w_s = 0.3$, $w_{p1} = 23.2$, $S_{a1} = 1$, $l_{a1} = 18$, $d = 0.4$, $h_1 = 0.813$, $h_2 = 0.813$, and $h_{air} = 2$.

extremely closely placed antennas. As shown in Fig. 4(c), the edge-to-edge distance between two antennas (d) is studied. According to the previous discussion, the mutual coupling is mainly decided by the alignment of the field, which is controlled by the offset between patches and cancellation of coupling, and the final decoupling performance is not very sensitive to the distance between patches. Stable −20 dB mutual coupling can still be guaranteed when two antennas are placed very close to each other, as shown in Fig. 4(c). When the patch separation is swept from 0.2 to 1.1 mm, the low mutual coupling is always maintained. The distance between two antennas can be even decreased, but a 0.5 mm distance is chosen for demonstration in this work after a compromise between performance and fabrication tolerance.

In this research, the stubs have been designed in a bent configuration to achieve a more compact size. However, straight stubs can lead to a further enhancement in the isolation performance. To demonstrate this, a design incorporating straight stubs has been developed and its parameters are provided in Fig. 5. The straight stubs provide an improvement of approximately 5 dB in the isolation performance in the relevant frequency range compared to the bent stub design. This is attributed to the fact that the electric field distribution of the straight stub design more closely aligns with the ideal scenario, as depicted in Fig. 2(c). Conversely, when the stubs are bent, the field distribution in the vicinity of the stubs becomes more complex, which can result in inevitable coupling between the open ends of the stubs and the adjacent patch. Therefore, there is a tradeoff between the achieved isolation performance and the occupied circuit area.

C. Cross-Polarization Suppression

In this section, the effect of the slots on the patches will be introduced. The simulated surface current distributions on the patches at the resonant frequency are shown in Fig. 6(a) when there are no slots etched on the patches. In the simulation, only the left-hand side antenna is excited. The current distributions indicate that the TM_{20} mode of the patch is excited by the probe. The out-of-phase current portion is shifted to the loading stubs. The narrow stubs contribute little to the radiation and current distribution on the dominating patch, similar to that of a classical TM_{10} mode. Besides, it can be observed that the current on the stub is stronger than the current on the main radiating patch. This asymmetric current distribution characteristic indicates that the stubs have a more substantial effect on the mutual coupling. As a result, regions *a* and *d* should be smaller than regions *b* and *c* to compensate for this effect.

The properly designed offset between two closely placed antennas makes them well-isolated. Only an extremely weak current can be found on the antenna on the right-hand side. However, when the excitation phase angle of the driven antenna is 90°, it is found that the current vectors on the right-hand side patch show component in the Y-direction.

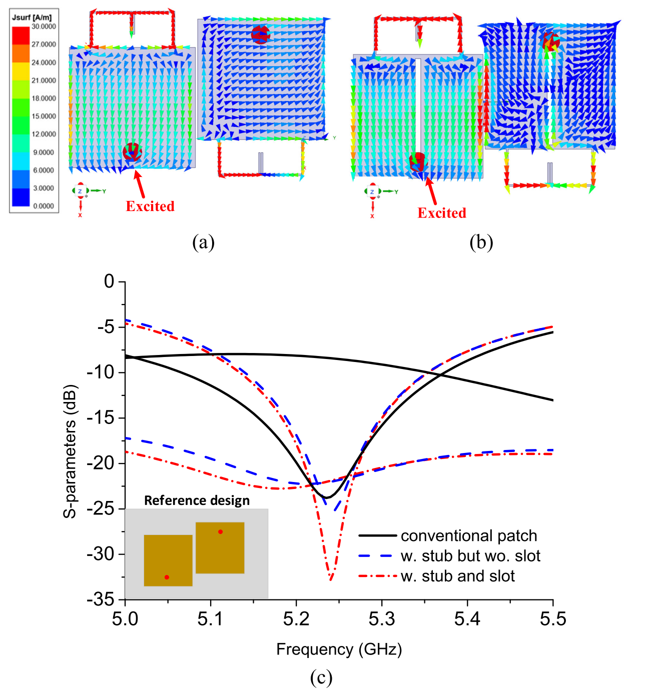

Fig. 6. (a) Surface current distributions on the patches without slots. (b) Surface current distributions on the patches with slots. (c) Simulated S-parameters for three different cases.

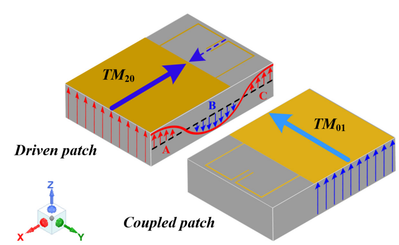

Fig. 7. Illustration for the field distributions of different modes.

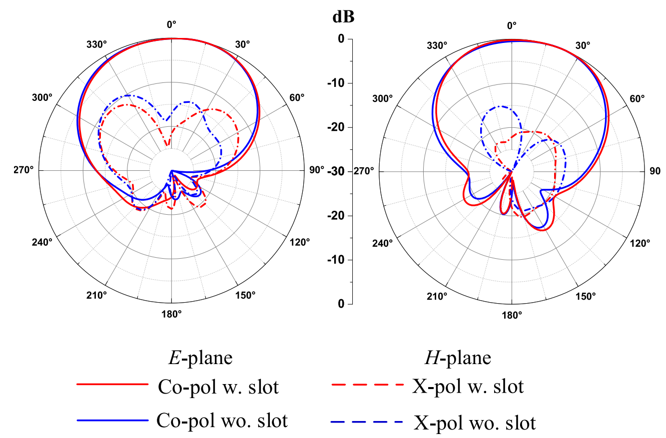

Fig. 8. Comparison of radiation patterns for antennas with/without loading slots.

This current will increase the cross-polarization, as shown in Fig. 6(a). The emergence of the Y component of the current on Ant. 2 is a result of the excitation of the TM_{01} mode of Ant. 2. As illustrated in Fig. 7, because of the offset between the two patches, the in-phase electrical field in region B will couple to the second patch and activates its TM_{01} mode. Thus, the activated TM_{01} mode of the second patch will radiate with polarization in the Y-direction. To mitigate this effect, a long narrow slot is cut at the center of the patch along with the direction of the polarization of the TM_{20} mode.

Fig. 6(b) shows the current distributions on the patches with slots. The incorporation of a long slot leads to a shift in the resonant frequency of the TM_{01} mode to a lower frequency band. Compared with the current distribution in Fig. 6(a), it can be observed that the slots have little effect on the original current behavior of the driven patch as the slot is etched in the same direction as the current of the TM_{20} mode. However, it can be observed that the current vectors in the Y-direction on the coupled patch are effectively suppressed.

The comparison of S-parameters for the cases with and without loading slots is presented in Fig. 6(c). A reference design featuring conventional rectangular patches operating over the first fundamental modes has also been evaluated. The interpatch distance and offset have been kept constant across all cases. The proposed technique demonstrates a significant improvement in isolation performance, with a 12 dB increase relative to the reference design utilizing classic patch antennas. Moreover, the loading slots exhibit a minimal impact on the S-parameters of the antenna module, which is consistent with the previous current studies. It is noteworthy to mention that the reference design, which operates over the TM_{10} modes, exhibits a wider impedance bandwidth. This can be attributed to the higher-order modes' higher quality factors compared to the first fundamental mode. Further investigation on the bandwidth improvement of a TM_{20} mode patch antenna will be carried out in future studies.

With these loading slots, the radiation from TM_{01} mode can be decreased. Hence, the cross-polarization that results from TM_{01} mode can be decreased too. Fig. 8 compares the radiation patterns for the antennas with and without slots. Benefiting from the loading slots, the cross-polarization levels in the broadside direction are decreased by about 5 dB for the H-plane, which is about 6 dB for the E-plane.

D. Measurement

To verify the concept, a prototype of the structure in Fig. 1 is fabricated and measured. The S-parameters are plotted in Fig. 9(a). A photograph of the fabricated antenna is also inset in Fig. 9(a). Very good in-band performance regarding impedance matching and bandwidths is observed. More specifically, the measured -10 dB impedance bandwidth is 5.14–5.35 GHz. Isolation between two antennas is higher than 20 dB across the operating band. With the mismatch loss considered, the measured radiation performance is plotted in Fig. 9(b). The measured total efficiency is higher than 84% in the band of interest. The measured realized gain at the broadside direction is 6.98 dBi at 5.25 GHz, which is 7.24 dBi for the simulation. The reasonable discrepancy between simulated and measured results can be attributed to fabrication tolerance and measurement errors.

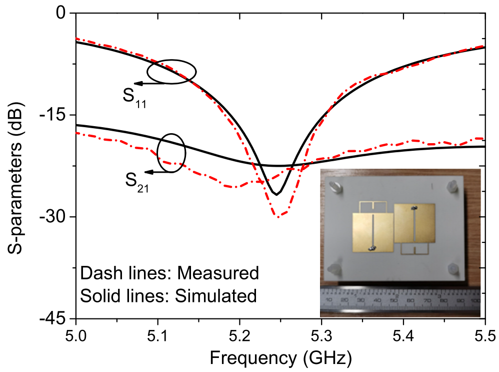

(a)

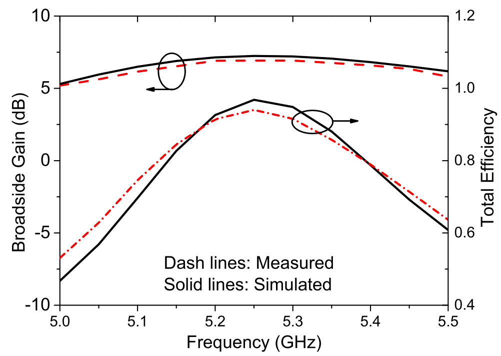

(b)

Fig. 9. Simulated and measured (a) S-parameters and (b) radiation performance for the dual-antenna system.

III. Application Prospects

In this section, two potential application prospects for the proposed decoupling method will be introduced with two design examples.

A. Four-Element MIMO Array

First, based on the results in Section II, this dual-antenna system can be easily scaled to a multiantenna MIMO system. In Fig. 10, a four-element MIMO antenna is illustrated for the demonstration of the potential of this method in MIMO applications. As can be observed, four antenna elements are placed extremely close to each other. The structure is rotationally symmetric, which means the geometry of Ant.1 (antenna 1) is the same as Ant. 4 and the geometry of Ant. 2 is the same as Ant. 3. Compared with Ant. 1, Ant. 2 is coupled with Ant. 1 and Ant. 3 simultaneously. So, there are some minor discrepancies in their sizes.

The simulated and measured *S*-parameters of the fabricated MIMO array are given in Fig. 11, together with an inserted photograph of the antennas. The measured decoupled bandwidth, with S_{11} and S_{22} < -10 dB and S_{12} < -20 dB, is 5.15–5.34 GHz. The measured realized gain at the broadside direction is 7.45 dBi at 5.25 GHz, which is 7.58 dBi for the simulation. The radiation patterns for the MIMO array at 5.25 GHz in the E- and H-planes are plotted in Fig. 12. Benefiting from the loading slots, the measured ratio between the co-polarization to cross-polarization is higher than 25 dB in the broadside direction. The measured 3 dB beamwidths for the E- and H-planes are 84° and 87°, respectively.

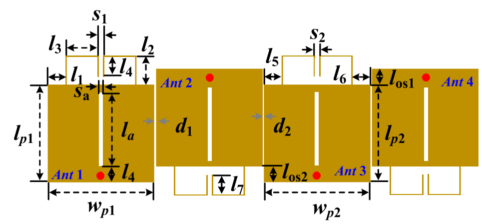

Fig. 10. Dimensions of the 4 × 4 MIMO array (unit: mm): $l_1 = 4.85$, $l_2 = 5.85$, $l_3 = 5.3$, $l_4 = 4.05$, $l_5 = 2.45$, $l_6 = 3.45$, $l_7 = 3.55$, $l_{os1} = 6$, $l_{os2} = 5.75$, $l_{p1} = 22.1$, $l_{p2} = 22.85$, $w_s = 0.3$, $w_{p1} = 22.4$, $w_{p2} = 21.8$, $S_a = 0.7$, $S_1 = 4.3$, $S_2 = 5.3$, $l_a = 16$, $d_1 = 1.4$, and $d_2 = 0.5$.

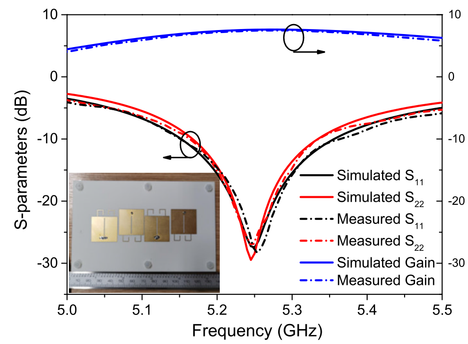

(a)

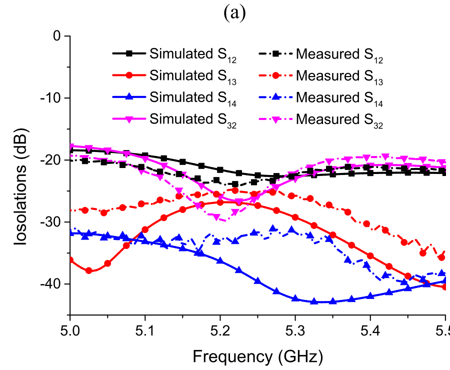

(b)

Fig. 11. Simulated and measured performance for the MIMO array. (a) Reflection coefficients and broadside gain. (b) Isolations.

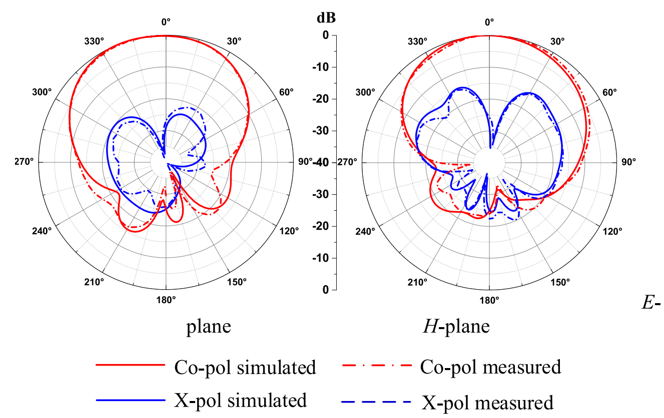

Fig. 12. Simulated and measured radiation patterns of the four-element MIMO array.

B. Adjacent-Band Decoupling

Another promising prospect of this method is that it can be applied for decoupling two antennas operating for two adjacent bands. In modern customer premises equipment (CPE),

TABLE I
COMPARISON OF THE PERFORMANCE BETWEEN DIFFERENT WORKS IN THE LITERATURE AND THIS WORK

Reference		Decoupling method	Antenna type	Edge-to-edge distance (λ_0)	Adjacent band operation	Isolation (dB)	Total efficiency	Array
[7]		Stacked Near-field resonators	Patch	0.016	N.V.	20	80	1 × 2
[12]		Network between antennas	Patch	0.2	N.V.	20	84%	2 × 2
[14]		Loaded resonator (Underneath the patch)	Patch	0.06	N.V.	23	N.G.	2 × 2
[19]		Weak-field-based	Patch	0.18	N.V.	29	N.G.	1 × 4
[20]		Mixed modes	Patch	0.12	N.V.	20	N.G.	1 × 2
[21]		Mode cancellation	Patch	0.016	N.V.	15.4	81%	1 × 2
[23]		Filtering structures	Patch	0.016	Yes	25	N.G.	N.A.
[24]		Filtering structure	N.G.	N.A.	Yes.	15	N.G.	N.A.
This work	In-band	Offset placement	Patch	0.007	N.A.	20.2	84%	1 × 2
	1 × 4 MIMO		Patch	0.02	N.A.	21.5	81%/	1 × 4
	Adjacent-band		Patch	0.011	Yes	20	83%/86%	N.A.

Note: λ_0 is the guided wavelength in the substrate at center frequency.
N. A.: Not applicable; N. V.: Not verified; N.G.: not given

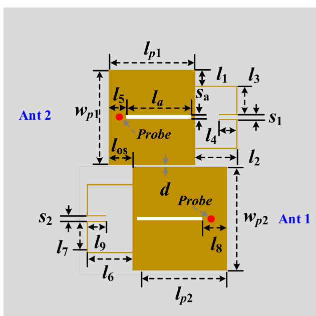

Fig. 13. Dimensions of the dual-antenna module with different operating bands. $l_1 = 3.8$, $l_2 = 6.675$, $l_3 = 7.4$, $l_4 = 3.725$, $l_5 = 3.2$, $l_6 = 6.675$, $l_7 = 7.4$, $l_8 = 4$, $l_9 = 4.425$, $l_{os} = 5.4$, $l_{p1} = 21.8$, $l_{p2} = 23.4$, $w_s = 0.3$, $w_p = 24.1$, $w_p = 26.1$, $S_a = 1$, $l_a = 18$, and $d = 0.7$ (unit: mm).

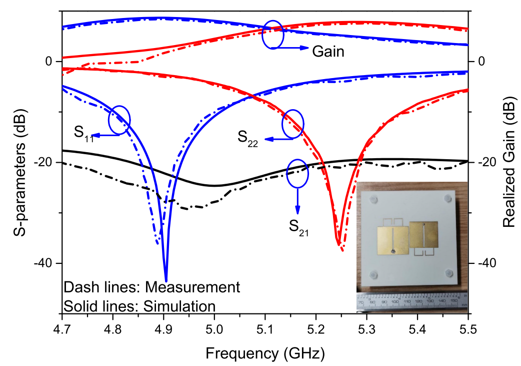

Fig. 14. Simulated and measured S-parameters and gain for the adjacent band operation design.

multiple standards should be simultaneously satisfied for WiFi and mobile communication. With all these antennas placed in a limited space, to make sure that the transmitted signal from one channel will not be received by the receiving channel of the other channel, the isolation between these antennas should be high enough, especially for two antennas operating over adjacent bands with very small guard band. As analyzed earlier, the decoupling mechanism of this method is achieved by designing coupling portions between antennas. One of its advantages is that it is still effective when both antennas operate at different frequency bands.

For demonstration, another design is developed based on the method presented in this work. The geometry of this dual-antenna system is shown in Fig. 13. Ant. 1 operates for the lower band, while Ant. 2 works for the higher band. Following the design guides introduced in Section II-B, the two antennas can be decoupled using the same method. The distance between two antennas is 0.7 mm in this case. The antennas were fabricated and measured with measured results plotted in Fig. 14. The measured −10 dB bandwidths for both antennas are 4.79–5.0 GHz and 5.13–5.37 GHz, respectively. The measured isolation in the band of interest is higher than 20 dB. The measured broadside gains for both antennas are 8.42 and 7.84 dBi, respectively. It should be noted here when two antennas are with different dimensions, the maximum gain will not arise at the $+z$-direction because of the asymmetric module structure. This scenario studies the case for two antennas operating for 5G band N79 (4400–5000 MHz) and 5 GHz WiFi band (5150–5925 MHz). Although the antennas in this case only cover part of these frequency bands, this design is still a good example, which demonstrates the adjacent-band decoupling ability of the proposed method.

C. Comparison and Discussion

The proposed decoupling method is compared with the state-of-the-art developments in the area in Table I. One of the most notable advantages of the proposed method is its ability to decouple two patch antennas with extremely close edge-to-edge distances. Additionally, the proposed method is unique in its capacity to address both in-band and adjacent-band decoupling issues and can be applied to multielement MIMO arrays. In contrast, other works either require the utilization of additional decoupling layers [7], [14] or demand a more involved design of decoupling structures [12], [23]. The proposed method, on the other hand, is comparatively simpler and does not necessitate the use of additional layers or interantenna decoupling elements, thereby making it a cost-effective and efficient design solution.

IV. Conclusion

This article has presented a novel method for the decoupling between extremely closely placed patch antennas. Patch antennas operating over its second mode (TM_{20}) have been utilized as the basic element of the multiantenna module. Isolations higher than 20 dB in the band of interest have been achieved by simply introducing an offset between antenna elements. Three different application scenarios have been studied in this work, demonstrating the effectiveness of the proposed method. Compared with other methods, the proposed technique has the advantage of structure simplicity and small edge-to-edge distance, which makes it a good candidate for future highly integrated communication systems.

Acknowledgment

The authors would like to thank Antonio Mendoza for support with measurements and Dr. Zhijiao Chen for technical discussions.

References

[1] P.-S. Kildal and K. Rosengren, "Correlation and capacity of MIMO systems and mutual coupling, radiation efficiency, and diversity gain of their antennas: Simulations and measurements in a reverberation chamber," *IEEE Commun. Mag.*, vol. 42, no. 12, pp. 104–112, Dec. 2004.

[2] K. E. Kolodziej, B. T. Perry, and J. S. Herd, "In-band full-duplex technology: Techniques and systems survey," *IEEE Trans. Microw. Theory Techn.*, vol. 67, no. 7, pp. 3025–3041, Jul. 2019.

[3] K. S. Vishvaksenan, K. Mithra, R. Kalaiarasan, and K. S. Raj, "Mutual coupling reduction in microstrip patch antenna arrays using parallel coupled-line resonators," *IEEE Antennas Wireless Propag. Lett.*, vol. 16, pp. 2146–2149, 2011.

[4] C.-Y. Chiu, C.-H. Cheng, R. D. Murch, and C. R. Rowell, "Reduction of mutual coupling between closely-packed antenna elements," *IEEE Trans. Antennas Propag.*, vol. 55, no. 6, pp. 1732–1738, Jun. 2007.

[5] K.-L. Wu, C. Wei, X. Mei, and Z.-Y. Zhang, "Array-antenna decoupling surface," *IEEE Trans. Antennas Propag.*, vol. 65, no. 12, pp. 6728–6738, Dec. 2017.

[6] Y.-F. Cheng, X. Ding, G.-F. Gao, W. Shao, and C. Liao, "Analysis and design of wide-scan phased array using polarization-conversion isolators," *IEEE Antennas Wireless Propag. Lett.*, vol. 18, no. 3, pp. 512–516, Mar. 2019.

[7] M. Li, B. G. Zhong, and S. W. Cheung, "Isolation enhancement for MIMO patch antennas using near-field resonators as coupling-mode transducers," *IEEE Trans. Antennas Propag.*, vol. 67, no. 2, pp. 755–764, Feb. 2019.

[8] S. N. Venkatasubramanian, L. Li, A. Lehtovuori, C. Icheln, and K. Haneda, "Impact of using resistive elements for wideband isolation improvement," *IEEE Trans. Antennas Propag.*, vol. 65, no. 1, pp. 52–62, Jan. 2017.

[9] H. Meng and K.-L. Wu, "An LC decoupling network for two antennas working at low frequencies," *IEEE Trans. Microw. Theory Techn.*, vol. 65, no. 7, pp. 2321–2329, Jul. 2017.

[10] Y.-F. Cheng and K.-K. M. Cheng, "A novel dual-band decoupling and matching technique for asymmetric antenna arrays," *IEEE Trans. Microw. Theory Techn.*, vol. 6, no. 5, pp. 2080–2089, May 2018.

[11] M. Li, M. Wang, L. Jiang, and K. L. Yeung, "Decoupling of antennas with adjacent frequency bands using cascaded decoupling network," *IEEE Trans. Antennas Propag.*, vol. 69, no. 2, pp. 1173–1178, Feb. 2021.

[12] Y.-M. Zhang, S. Zhang, J.-L. Li, and G. F. Pedersen, "A transmission-line-based decoupling method for MIMO antenna arrays," *IEEE Trans. Antennas Propag.*, vol. 67, no. 5, pp. 3117–3131, May 2019.

[13] B. Tütüncü, "Mutual coupling reduction using coupling matrix based band stop filter," *AEU Int. J. Electron. Commun.*, vol. 124, Sep. 2020, Art. no. 153342.

[14] Y.-F. Cheng and K.-K.-M. Cheng, "Decoupling of 2 × 2 MIMO antenna by using mixed radiation modes and novel patch element design," *IEEE Trans. Antennas Propag.*, vol. 69, no. 12, pp. 8204–8213, Dec. 2021.

[15] X. Gao, H. Zhong, Z. Zhang, Z. Feng, and M. F. Iskander, "Low-profile planar tripolarization antenna for WLAN communications," *IEEE Antennas Wireless Propag. Lett.*, vol. 9, pp. 83–86, 2010.

[16] K. Zhang, Z. H. Jiang, W. Hong, and D. H. Werner, "A low-profile and wideband triple-mode antenna for wireless body area network concurrent on-/off-body communications," *IEEE Trans. Antennas Propag.*, vol. 68, no. 3, pp. 1982–1994, Mar. 2020.

[17] K.-L. Wong, J.-Z. Chen, and W.-Y. Li, "Four-port wideband annular-ring patch antenna generating four decoupled waves for 5G multi-input–multi-output access points," *IEEE Trans. Antennas Propag.*, vol. 69, no. 5, pp. 2946–2951, May 2021.

[18] A. Zhang, K. Wei, Y. Hu, and Q. Guan, "High-isolated coupling-grounded patch antenna pair with shared radiator for the application of 5G mobile terminals," *IEEE Trans. Antennas Propag.*, vol. 70, no. 9, pp. 7896–7904, Sep. 2022.

[19] H. Lin, Q. Chen, Y. Ji, X. Yang, J. Wang, and L. Ge, "Weak-field-based self-decoupling patch antennas," *IEEE Trans. Antennas Propag.*, vol. 68, no. 6, pp. 4208–4217, Jun. 2020.

[20] Q. X. Lai, Y. M. Pan, S. Y. Zheng, and W. J. Yang, "Mutual coupling reduction in MIMO microstrip patch array using TM10 and TM02 modes," *IEEE Trans. Antennas Propag.*, vol. 69, no. 11, pp. 7562–7571, Nov. 2021.

[21] L. Sun, Y. Li, and Z. Zhang, "Decoupling between extremely closely spaced patch antennas by mode cancellation method," *IEEE Trans. Antennas Propag.*, vol. 69, no. 6, pp. 3074–3083, Jun. 2021.

[22] Y. Zhang, X. Y. Zhang, L.-H. Ye, and Y.-M. Pan, "Dual-band base station array using filtering antenna elements for mutual coupling suppression," *IEEE Trans. Antennas Propag.*, vol. 64, no. 8, pp. 3423–3430, Aug. 2016.

[23] J. Guo, F. Liu, L. Zhao, G.-L. Huang, Y. Li, and Y. Yin, "Isolation improvement of two tightly coupled antennas operating in adjacent frequency bands using filtering structures," *IEEE Open J. Antennas Propag.*, vol. 1, pp. 207–214, 2020.

[24] L. Zhao, F. Liu, X. Shen, G. Jing, Y.-M. Cai, and Y. Li, "A high-pass antenna interference cancellation chip for mutual coupling reduction of antennas in contiguous frequency bands," *IEEE Access*, vol. 6, pp. 38097–38105, 2018.

[25] K.-F. Lee, K. Ho, and J. Dahele, "Circular-disk microstrip antenna with an air gap," *IEEE Trans. Antennas Propag.*, vol. AP-32, no. 8, pp. 880–884, Aug. 1984.

[26] J.-F. Qian, F.-C. Chen, and Q.-X. Chu, "A novel tri-band patch antenna with broadside radiation and its application to filtering antenna," *IEEE Trans. Antennas Propag.*, vol. 66, no. 10, pp. 5580–5585, Oct. 2018.

[27] A. A. Deshmukh and K. P. Ray, "Multi-band configurations of stub-loaded slotted rectangular microstrip antennas," *IEEE Antennas Propag. Mag.*, vol. 52, no. 1, pp. 89–103, Feb. 2010.

[28] J.-D. Zhang, L. Zhu, N.-W. Liu, and W. Wu, "Dual-band and dual-circularly polarized single-layer microstrip array based on multiresonant modes," *IEEE Trans. Antennas Propag.*, vol. 65, no. 3, pp. 1428–1433, Mar. 2017.

[29] Q. Tan and F.-C. Chen, "Triband circularly polarized antenna using a single patch," *IEEE Antennas Wireless Propag. Lett.*, vol. 19, no. 12, pp. 2013–2017, Dec. 2020.

[30] ANSYS Inc. *ANSYS HFSS*. Accessed: 2017. [Online]. Available: http://www.ansys.com/Products/Electronics/ANSYS-HFSS

Jian-Feng Qian (Graduate Student Member, IEEE) received the B.S. degree from the Hefei University of Technology, Hefei, China, in 2016, and the M.E. degree from the South China University of Technology, Guangzhou, China, in 2019. He is currently pursuing the Ph.D. degree with the University of Kent, Canterbury, U.K.

His research interests include microwave antennas, filters, filtering antennas, and associated RF circuits for microwave and millimeter-wave applications.

Mr. Qian was twice awarded the China National Scholarship for Postgraduates in 2017 and 2018. In 2019, he was awarded the Outstanding Graduate Student of Guangdong Province. He was a recipient of the Outstanding Master's Thesis Award from the Chinese Institute of Electronics, in 2019 and the Best Student Paper Award from the 17th International Workshop on Antenna Technology (iWAT 2022), Dublin.

Steven Gao (Fellow, IEEE) received the Ph.D. degree from Shanghai University, Shanghai, China, in 1991.

He was a Chair Professor with the University of Kent, Kent, U.K., for nearly ten years. He is currently a Professor with the Department of Electronic Engineering, The Chinese University of Hong Kong, Hong Kong. He has coauthored or coedited three books *Space Antenna Handbook* (Wiley, 2012), *Circularly Polarized Antennas* (IEEE and Wiley, 2014), and *Low-Cost Smart Antennas* (Wiley, 2019); more than 400 articles; and holds 20 patents. His current research interests include smart antennas, phased arrays, multi-in-multi-out (MIMO), reconfigurable antennas, broadband/multiband antennas, satellite antennas, RF/microwave/millimeter-wave/terahertz circuits, mobile communications, satellite communications, ultrawideband (UWB) radars, synthetic aperture radars, sensors, the Internet of Things (IoT), and small satellites.

Dr. Gao is a Fellow of the Royal Aeronautical Society, U.K., and IET, U.K. He is the U.K./Ireland Representative with the European Association on Antennas and Propagation (EurAAP). He was the General Chair of Loughborough Antennas and Propagation Conference (LAPC) 2013 and an Invited/Keynote Speaker at many conferences. He was a Distinguished Lecturer of the IEEE Antennas and Propagation Society and serves as an Associate Editor for several international journals (IEEE TRANSACTIONS ON ANTENNAS AND PROPAGATION, *Radio Science Electronics Letters*, and *IET Circuits, Devices and Systems*) and the Editor-in-Chief for John Wiley and Sons Book Series on *Microwave and Wireless Technologies*. He served as the Lead Guest Editor for the Special Issue on Small Satellites of the PROCEEDINGS OF THE IEEE in 2018, the Lead Guest Editor for the Special Issue on Antennas for Satellite Communication of the IEEE TRANSACTIONS ON ANTENNAS AND PROPAGATION in 2015, and the Guest Editor for the Special Issue on Photonic and RF Communications Systems of *IET Circuits, Devices and Systems* in 2014.

Benito Sanz-Izquierdo (Member, IEEE) received the B.Sc. degree from ULPGC, Las Palmas, Spain, and the M.Sc. and Ph.D. degrees from the University of Kent, Canterbury, U.K.

He was a Research Associate with the School of Engineering, University of Kent, where he became a Lecturer in electronic systems in 2013, and a Senior Lecturer in 2018. In 2012, he worked at Harada Industries Ltd., where he developed novel antennas for the automotive industry. His research interests include multiband antennas, wearable electronics, additive manufacturing (3-D printing), substrate integrated waveguides components, metamaterials, sensors, electromagnetic bandgap structures, frequency-selective surfaces, and reconfigurable devices.

Hanyang Wang (Fellow, IEEE) received the Ph.D. degree from Heriot-Watt University, Edinburgh, U.K., in 1995.

From 1986 to 1991, he served as a Lecturer and an Associate Professor with Shandong University, Jinan, China. From 1995 to 1999, he was a Post-Doctoral Research Fellow with the University of Birmingham, Birmingham, U.K., and the University of Essex, Colchester, U.K. From 1999 to 2000, he was a Software Development and Microwave Engineering Consultant Engineer with Vector Fields Ltd., Oxford, U.K. He joined Nokia U.K. Ltd., Farnborough, U.K., in 2001, where he was a Mobile Antenna Specialist for 11 years. He joined Huawei Technologies, Reading, U.K., and he is currently the Chief Mobile Antenna Expert and the Head of the Mobile Antenna Technology Division, Huawei. He is also an Adjunct Professor with the School of Electronics and Information Technology, Sichuan University, Chengdu, China. He has authored over 100 refereed articles on these topics. He holds over 50 granted and pending US/EU/CN patents. His current research interests include small and multiband antennas for mobile terminals, antennas and antenna arrays for 5G mobile communications, and numerical methods for the solutions of electromagnetic radiation and scattering problems.

Dr. Wang is a Huawei Fellow and an IET Fellow. He was a recipient of the Title of Nokia Inventor of the Year in 2005, the Nokia Excellence Award in 2011, the Huawei Individual Gold Medal Award in 2012, and the Huawei Team Gold Medal Award in 2013 and 2014, respectively. His patent was ranked number one among 2015 Huawei top ten patent awards. He is an Associate Editor of the IEEE ANTENNAS AND WIRELESS PROPAGATION LETTERS.

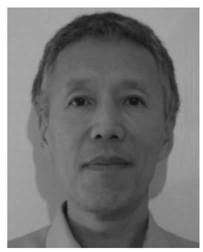

Hai Zhou received the Ph.D. degree in reflector antenna synthesis from the University of London, London, U.K., in 1987.

He carried out his post-doctoral work with the University of London, until 1992. He served as a Senior Lecturer with London South Bank University, London, working on global system for mobile communications (GSM), universal mobile telecommunications service (UMTS), and LTE in system engineering. He joined Lucent Technologies, Wiltshire, U.K., in 1996. He joined Huawei Technologies, Reading, U.K., in 2015. He worked on various topics from shaped reflector antenna synthesis, FDTD during his academic years to radio resource management and adaptive antennas in industry. He has authored or coauthored 14 journal articles and 34 conference papers. He holds 18 patents.

Dr. Zhou was a recipient of the Best Paper Award from the 19th European Microwave Conference in 1989 and received the Oliver Lodge Premium from IEE as the Best Paper of the Year on antennas and propagation in 1991.

Huiliang Xu was born in Leshan, Sichuan, China. He received the B.S. degree in applied geophysics from the China University of Mining and Technology, Xuzhou, Jiangsu, China, in 1998, the M.S. degree in optics from South China Normal University, Guangzhou, China, in 2005, and the Ph.D. degree in optical engineering from the Institute of Optics and Electronics, Chinese Academy of Sciences, Chengdu, Sichuan, China, in 2008.

From 1998 to 2002, he was a Petroleum Logging Engineer with China Petroleum Logging Company Ltd., Xi'an, China. In October 2008, he joined Huawei Technologies Company Ltd., Shenzhen, China, where he is the Wireless Terminal Antenna Expert. His current research interests include metal reconfigurable antenna, wearable antennas, vehicle-mounted antenna, metamaterial antenna, and antenna system simulation.